Molecular Cell

Volume 10 Number 6 December 2002

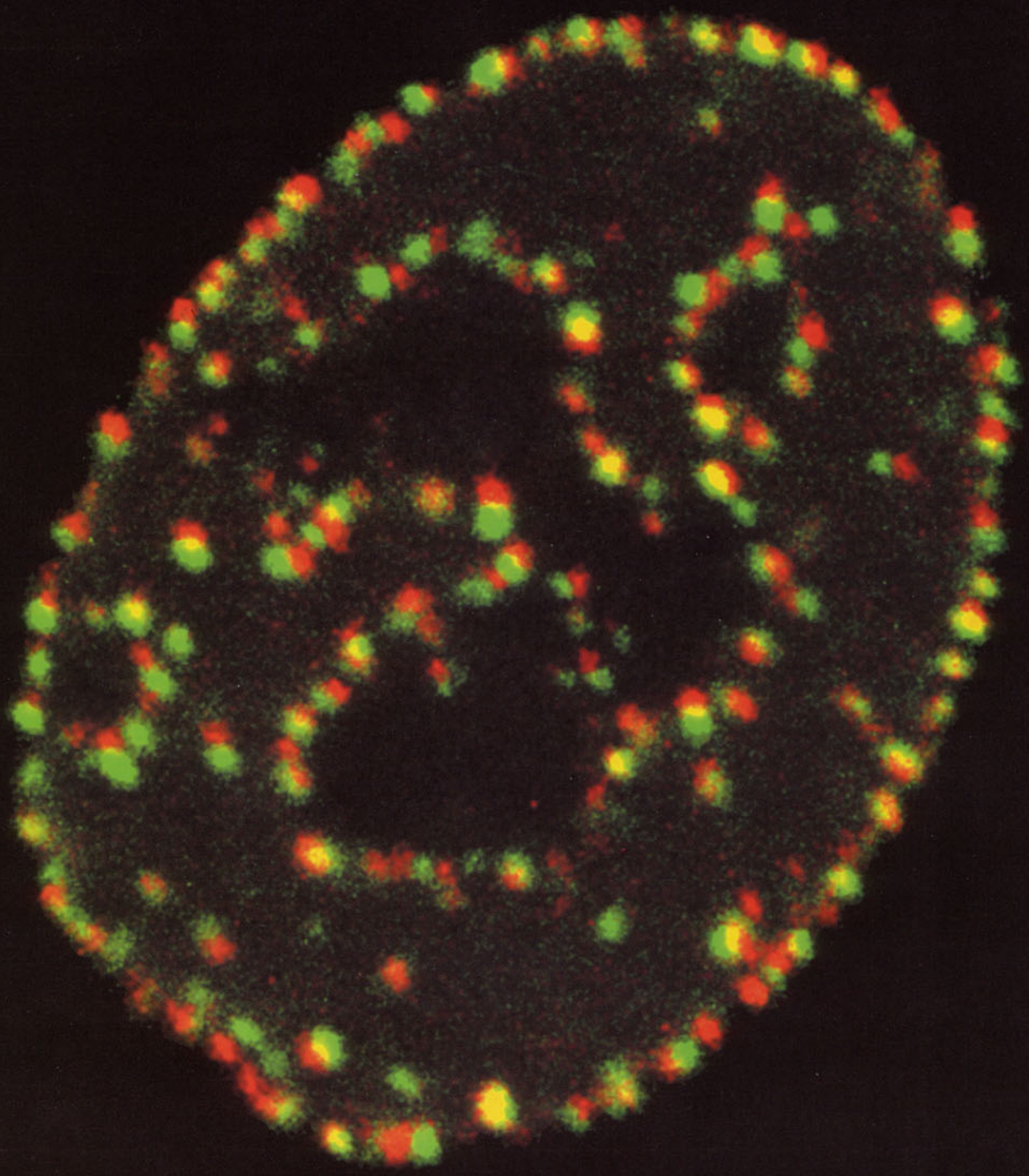

Propagation of DNA Replication

Molecular Cell, Vol. 10, 1355–1365, December, 2002, Copyright ©2002 by Cell Press

DNA Polymerase Clamp Shows Little Turnover at Established Replication Sites but Sequential De Novo Assembly at Adjacent Origin Clusters

Anje Sporbert,[1] Anja Gahl,[1] Richard Ankerhold,[2] Heinrich Leonhardt,[1,3,5] and M. Cristina Cardoso[1,4,5]
[1]Max Delbrück Center for Molecular Medicine
13125 Berlin
[2]Carl Zeiss Jena GmbH
Advanced Imaging Microscopy
07745 Jena
[3]Ludwig Maximilians University
Department of Biology II
80336 Munich
Germany

Summary

The spatial and temporal organization of DNA replication was investigated in living cells with a green fluorescent protein fusion to the DNA polymerase clamp PCNA. In situ extractions and photobleaching experiments revealed that PCNA, unlike RPA34, shows little if any turnover at replication sites, suggesting that it remains associated with the replication machinery through multiple rounds of Okazaki fragment synthesis. Photobleaching analyses further showed that the transition from earlier to later replicons occurs by disassembly into a nucleoplasmic pool of rapidly diffusing subcomponents and reassembly at newly activated sites. The fact that these replication sites were de novo assembled in close proximity to earlier ones suggests that activation of neighboring origins may occur by a domino effect possibly involving local changes in chromatin structure and accessibility.

Introduction

The basic mechanisms of DNA replication have been elucidated mostly by biochemical and genetic studies. At the molecular level, at least two different DNA polymerases, a DNA helicase, a single-stranded DNA binding protein complex (replication protein A, RPA), a clamp loading complex (replication factor C, RFC), a polymerase clamp (proliferating cell nuclear antigen, PCNA), nucleases, a DNA ligase, and DNA topoisomerases cooperate to replicate the DNA template (Waga and Stillman, 1994). Due to the polarity of the DNA synthesis reaction, at each replication fork, in addition to the continuous leading strand synthesis, a rather complex discontinuous synthesis of the lagging strand takes place involving the coordination of several different enzymatic activities (reviewed in Hubscher and Seo, 2001). To explain how the synthesis of both strands is coordinated, an asymmetric dimer of DNA polymerases and associated factors has been proposed for prokaryotic DNA replication (McHenry, 1988) and extended for eukaryotes (Tsurimoto and Stillman, 1989). To explain how the dimeric polymerases can extend the two antiparallel strands in the same direction and at the same rate, looping back of the lagging strand into the replisome ("trombone" model) has been postulated, with recycling of the lagging strand polymerase from the end of one Okazaki fragment to the next RNA primer (Sinha et al., 1980). Electron microscopic studies with purified phage T7 proteins have provided evidence for the existence of such loops (Lee et al., 1998), and biochemical studies with *Escherichia coli* DNA polymerase have suggested that the lagging strand polymerase remains associated via protein-protein interactions with the replication fork through multiple rounds of Okazaki fragment synthesis (Wu et al., 1992). The processivity of DNA polymerases is enhanced by association with a sliding clamp, which in eukaryotes is a homotrimeric PCNA ring encircling the DNA (Gulbis et al., 1996; Krishna et al., 1994; Schurtenberger et al., 1998). This ring is thought to act as a central loading platform for many enzymes involved in the duplication of genetic and epigenetic information. PCNA is essential for the coordinated synthesis of leading and lagging strand (Prelich and Stillman, 1988). According to a recent model, a new PCNA clamp is loaded at each Okazaki fragment (i.e., in eukaryotes, about every 180 bp) by RFC and may remain on replicated DNA marking the lagging strand and coordinating the multiple steps of its maturation (Shibahara and Stillman, 1999). At present, little if anything is known about the dynamic composition of the leading and lagging strand machinery in living cells. It is suggestive, although not proven, that one stable and processive polymerase complex synthesizes the leading strand from beginning to end. The complex nature of the discontinuous synthesis of the lagging strand, however, poses numerous challenges. The main question is whether one PCNA ring remains stably associated with the replication machinery, allowing the synthesis and maturation of only one Okazaki fragment at a time, or whether for each Okazaki fragment a new PCNA ring is loaded, allowing the maturation of multiple Okazaki fragments in parallel and a faster progression of the replication machinery.

At the cellular level, eukaryotic DNA replication takes place at microscopically visible subnuclear sites called replication foci (Nakamura et al., 1986) consisting of clusters of replicons and their associated replication machines (replisomes), which become activated in a coordinated manner (reviewed in Berezney et al., 2000). The existence of replication foci in living mammalian cells has been demonstrated using fusions of DNA ligase I and PCNA to GFP (Cardoso et al., 1997; Leonhardt et al., 2000; Somanathan et al., 2001). It has been estimated that eukaryotic chromosomal DNA comprises thousands of replicons (Huberman and Riggs, 1968), all of which become activated at specific times during S phase (Goldman et al., 1984; Lima-de-Faria and Jaworska, 1968). Using cell-free systems, the replication timing of mammalian chromosomal domains was shown to be established in early G1, after prereplication complex binding and concomitantly with the global repositioning of chromosomes within the nucleus (Dimitrova and Gilbert, 1999). The mechanistic basis of this temporal and

[4]Correspondence: cardoso@mdc-berlin.de
[5]These authors contributed equally to this work.

spatial organization of DNA replication remains unknown and requires either thousands of replisomes to be assembled and disassembled or a direct reuse of assembled replisomes throughout S phase.

The subnuclear patterns of replication foci visualized with GFP-tagged PCNA were shown by time lapse microscopy to change continuously throughout S phase in nuclei of living cells (Leonhardt et al., 2000; Somanathan et al., 2001). This change of replication foci pattern is not due to movement of entire replication foci from one position within the nucleus to another one as shown for other subnuclear structures like the Cajal bodies (Boudonck et al., 1999; Sleeman and Lamond, 1999), but is probably due to disassembly and reassembly at new sites (Leonhardt et al., 2000). Replication foci consist of clusters of replisomes, each being a large macromolecular complex containing all the activities necessary for the complete duplication of one replicon. That raises the question of whether entire replisomes within one cluster move from one replicon to the next or whether they disassemble into individual proteins or into small complexes. It is also not known when during the cell cycle, where in the nucleus, and how these complexes are assembled. Large multiprotein replication complexes have been biochemically isolated from mammalian cells (Noguchi et al., 1983; Tom et al., 1996; Wu et al., 1994), but it is unclear whether they were derived from the nucleoplasmic pool or from replication foci. Moreover, it is not known how replication factors reach their sites of action: freely moving through the nucleus, constrained by nuclear structures, or actively recruited.

To directly probe the nuclear dynamics of replication factors throughout the cell cycle in living mammalian cells we used a cell line expressing the GFP-tagged polymerase clamp PCNA and analyzed its association with replication sites by biochemical in situ extractions and by fluorescence photobleaching combined with time lapse microscopy.

Results

GFP-PCNA, Like the Endogenous PCNA, Binds Tightly to Sites of Ongoing DNA Replication

To investigate the dynamics of replication factors throughout the cell cycle, a stable C2C12 myoblast cell line was generated expressing GFP-PCNA and used throughout all experiments. In this stable cell line, low levels of fusion protein are expressed that do not affect cell cycle progression (Leonhardt et al., 2000). The GFP-PCNA-expressing cells show a cell cycle-dependent subnuclear distribution of the GFP fusion protein. As its endogenous counterpart, GFP-PCNA shows a diffuse distribution in nuclei of non-S phase cells while in S phase nuclei, changing patterns of nuclear foci appear (Leonhardt et al., 2000). Previous results also show that GFP-PCNA accurately labels sites of ongoing DNA replication as GFP-PCNA foci colocalize with sites of BrdU in S phase cells (Leonhardt et al., 2000).

To compare the subnuclear association properties of the GFP fusion protein with the endogenous PCNA in situ salt extraction experiments prior to fixation were performed in the parental C2C12 cell line and in the GFP-PCNA-expressing cell line (Figure 1). As shown by immunofluorescence stainings, PCNA is extracted from the nuclei of non-S phase cells with 150 mM NaCl. In S phase nuclei identified by BrdU incorporation, it remained associated with replication sites under these conditions (data not shown). Even after extraction with 300 or 500 mM NaCl, typical S phase patterns of PCNA are observed (Figure 1A), indicating a tight association

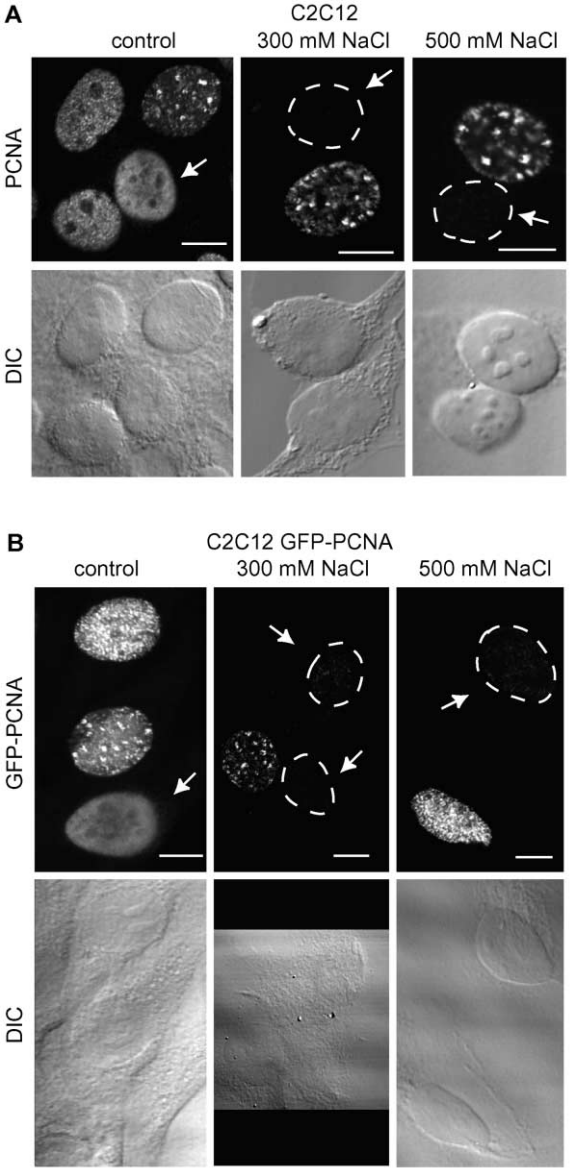

Figure 1. GFP-PCNA, Like the Endogenous PCNA, Binds Tightly to DNA Replication Foci during S Phase

(A) Distribution of endogenous PCNA (detected by immunofluorescence) and (B) GFP-PCNA in untreated asynchronous populations of C2C12 cells (control) and after extraction of the cells with 300 or 500 mM NaCl for 1 min. In untreated cells, both endogenous PCNA and GFP-PCNA are readily visible in non-S (see arrows in [A] and [B]) and S phase cells. Upon in situ extraction with salt concentrations up to 500 mM NaCl prior to fixation, only the proteins associated to replication sites are bound and visible while proteins in non-S phase nuclei are extracted. Scale bars, 10 μm.

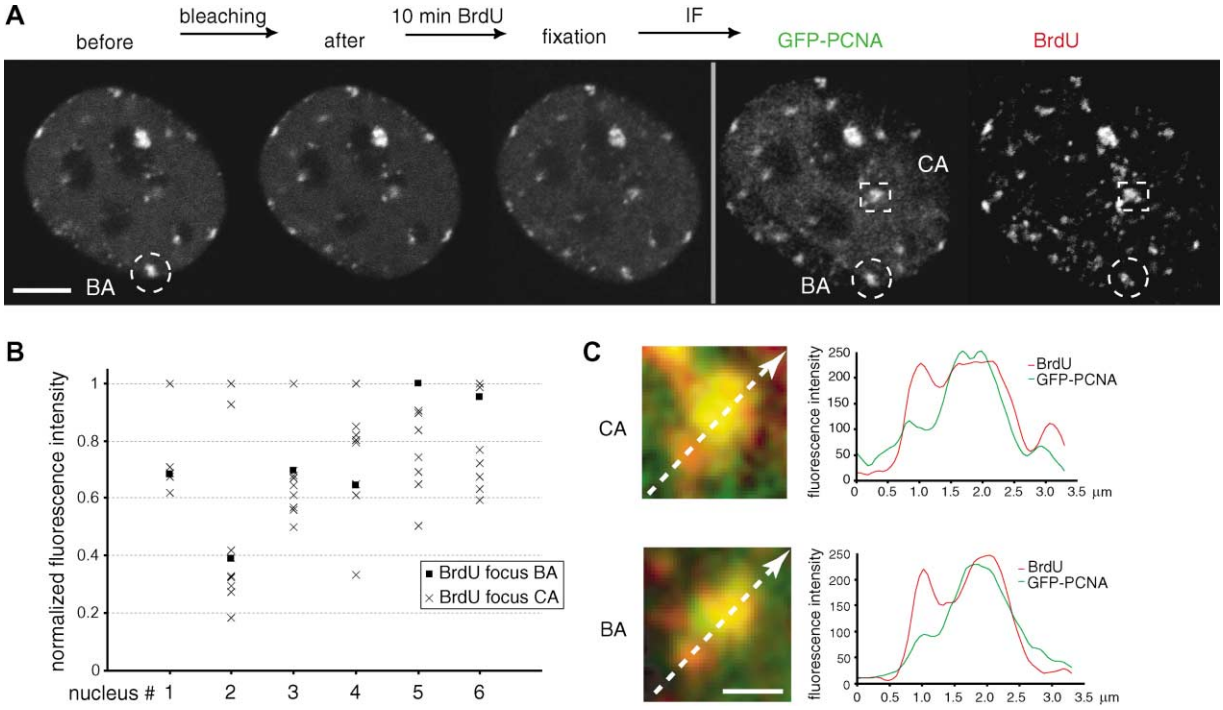

Figure 2. Photobleaching of GFP-PCNA at Replication Foci Does Not Alter Replicational Activity nor Does It Impair De Novo Assembly of GFP-PCNA

In S phase nuclei of living cells, one GFP-PCNA focus was bleached (BA), and immediately after, BrdU was added to the culture medium for 10 min.

(A) Confocal sections of one representative experiment show the nucleus before and after photobleaching, the fixed nucleus after BrdU pulse and after immunofluorescence staining (IF) of BrdU. The bleached GFP-PCNA focus recovered fluorescence during the 10 min BrdU pulse. The corresponding BrdU pattern indicates that DNA synthesis is not impaired by photobleaching. Scale bar, 5 μm.

(B) The fluorescence intensity of BrdU incorporated during the 10 min period after photobleaching into foci (n = 6–12 for each nucleus) of the bleached area (BA) and of the unbleached area (CA) was measured in several nuclei (n = 6) at different S phase stages. The amount of incorporated BrdU of bleached foci is within the range given by foci in the CA of the same nucleus indicating no alteration of replicational activity.

(C) Magnification of overlayed GFP-PCNA and BrdU of the BA and the CA. The fluorescence intensities measured along a line show in both areas adjacent sites with high amounts of BrdU but less GFP-PCNA and sites with high concentrations of both. Scale bar, 1 μm. The former areas represent newly replicated chromatin ("newborn" DNA) from which PCNA has already disassembled (see Figure 5).

of the protein with replication sites. The GFP fusion protein is like its endogenous counterpart extractable from non-S phase cells at low salt concentrations (150 mM NaCl, data not shown). Again, typical S phase patterns of GFP-PCNA remain visible even after extraction with 300 and 500 mM NaCl (Figure 1B) as well as after longer extraction times (data not shown). Taken together these results show that the GFP fusion protein accurately labels sites of ongoing DNA replication and exhibits a cell cycle-dependent tight association with replication sites indistinguishable from the endogenous PCNA.

Dynamics of GFP-PCNA at Sites of DNA Replication

Replication foci appear as rather stable structures over a period of 30 min to sometimes several hours (Leonhardt et al., 2000). Recently, the concept of stable subnuclear structures has been challenged by the finding that other apparently stable structures (e.g., speckled compartment) seem to be in constant flux, i.e., the movement of factors in and out of these structures takes place at the same rate as the movement of the nucleoplasmic pool of these factors (Kruhlak et al., 2000; Phair and Misteli, 2000; reviewed in Misteli, 2001; Pederson, 2000; Shopland and Lawrence, 2000).

To investigate whether and how fast replication factors move into and out of sites of DNA replication, we performed fluorescence photobleaching experiments on replication foci of S phase nuclei.

First, incorporation of the nucleotide analog BrdU was analyzed to test whether photobleaching of replication foci impairs DNA synthesis. Figure 2A shows a confocal z section of a living late S phase nucleus before and after photobleaching. Immediately after photobleaching, the cells were incubated with BrdU for 10 min to label sites of active DNA synthesis. Subsequent immunofluorescence staining showed incorporation of BrdU in the bleached focus as well as in unbleached replication foci, demonstrating that bleaching does not impair DNA synthesis neither at bleached nor at unbleached sites. Also longer times after photobleaching were examined, and no impairment of DNA replication was observed (data not shown). Several other nuclei were treated similarly and the replicational activity (fluorescence intensity of incorporated BrdU) at bleached and unbleached foci quantified (Figure 2B). Notwithstanding the large variability of

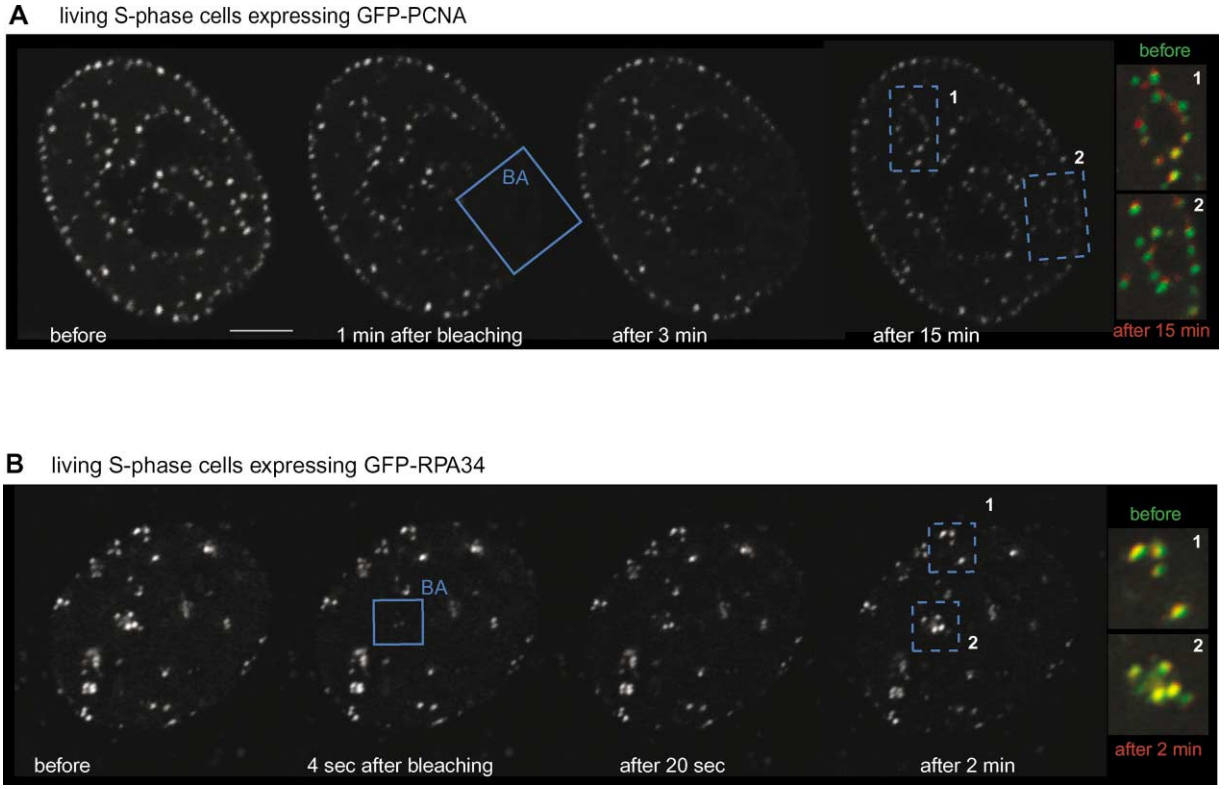

Figure 3. PCNA and RPA34, Two Factors Involved in DNA Replication, Show Different Fluorescence Recovery Behavior at Replication Sites

In live S phase cells expressing GFP-PCNA (A) or GFP-RPA34 (B), an area containing several replication foci was photobleached. Stacks of images were acquired before bleaching and at several time points after photobleaching to follow the fluorescence recovery. (A) GFP-PCNA assembled at replication foci shows no fluorescence recovery within 1 min after photobleaching. A slight recovery occurs first after 3 min, being clearly visible after several more minutes. In contrast, GFP-RPA34 (B) recruited to replication foci shows a slight fluorescence recovery already about 4 s after photobleaching, being clearly visible after 20 s and still increasing until 2 min after photobleaching (later time points not shown). The insets in (A) and (B) show time overlays of a bleached (2) and an unbleached region (1) of the prebleach image (in green) and an image after fluorescence recovery (in red). In contrast to GFP-PCNA, GFP-RPA34 exhibits a fast recovery (within seconds as opposed to several minutes for GFP-PCNA) at the bleached replication foci. Scale bar, 5 μm.

the amount of incorporated BrdU among foci in one nucleus and between nuclei, the bleached foci showed no altered DNA synthetic activity.

In an early/mid S phase and in a late S phase nucleus expressing GFP-PCNA, an area containing several replication foci (BA, about one-fifth or one-fourth of the nucleus) was bleached (Figure 3A and see Supplemental Figure S1 at http://www.molecule.org/cgi/content/full/10/6/1355/DC1). Directly after bleaching (1 min), an image of the bleached z section was acquired followed by several z stacks at various time points (3–25 min) after bleaching. During this time the bleached foci showed a fluorescence recovery while the unbleached foci decreased their initial fluorescence ending up in a similar intensity range as the bleached foci. When compared with the fast kinetics of recovery of the nucleoplasmic pool of GFP-PCNA where full recovery was observed in less than 3 s (see Supplemental Figures S2E–S2H at http://www.molecule.org/cgi/content/full/10/6/1355/DC1), GFP-PCNA at replication foci showed a strikingly stable association, in agreement with the in situ extraction results (Figure 1).

In order to rule out any methodological problems, we then compared the turnover of GFP-PCNA at replication sites with another replication factor, the single-stranded DNA binding protein RPA34, which plays a very different role in DNA replication. RPA34 binds in a heterotrimeric complex the unwound DNA during the initiation of DNA replication, coating the single strands and stabilizing the open DNA conformation. C2C12 myoblasts expressing a fusion of GFP to the human RPA34 (GFP-RPA34; for characterization of the fusion protein see Supplemental Figure S3 at http://www.molecule.org/cgi/content/full/10/6/1355/DC1) were analyzed using the same conditions as with GFP-PCNA. In stark contrast to GFP-PCNA, GFP-RPA34-labeled replication foci showed a rather fast fluorescence recovery within seconds, reaching a maximum at about 1–2 min (Figure 3B). The very different recovery kinetics of these two replication factors at sites of DNA replication measured under the same conditions clearly establishes that the slow recovery of GFP-PCNA is a specific feature of PCNA.

Although GFP-PCNA shows a relatively slow fluorescence recovery, indicating a stable association with replication sites, the amount of fluorescence recovered at about 15 min after photobleaching is considerable (see Figures 2A and 3A and Supplemental Figure S1 at http://www.molecule.org/cgi/content/full/10/6/1355/DC1).

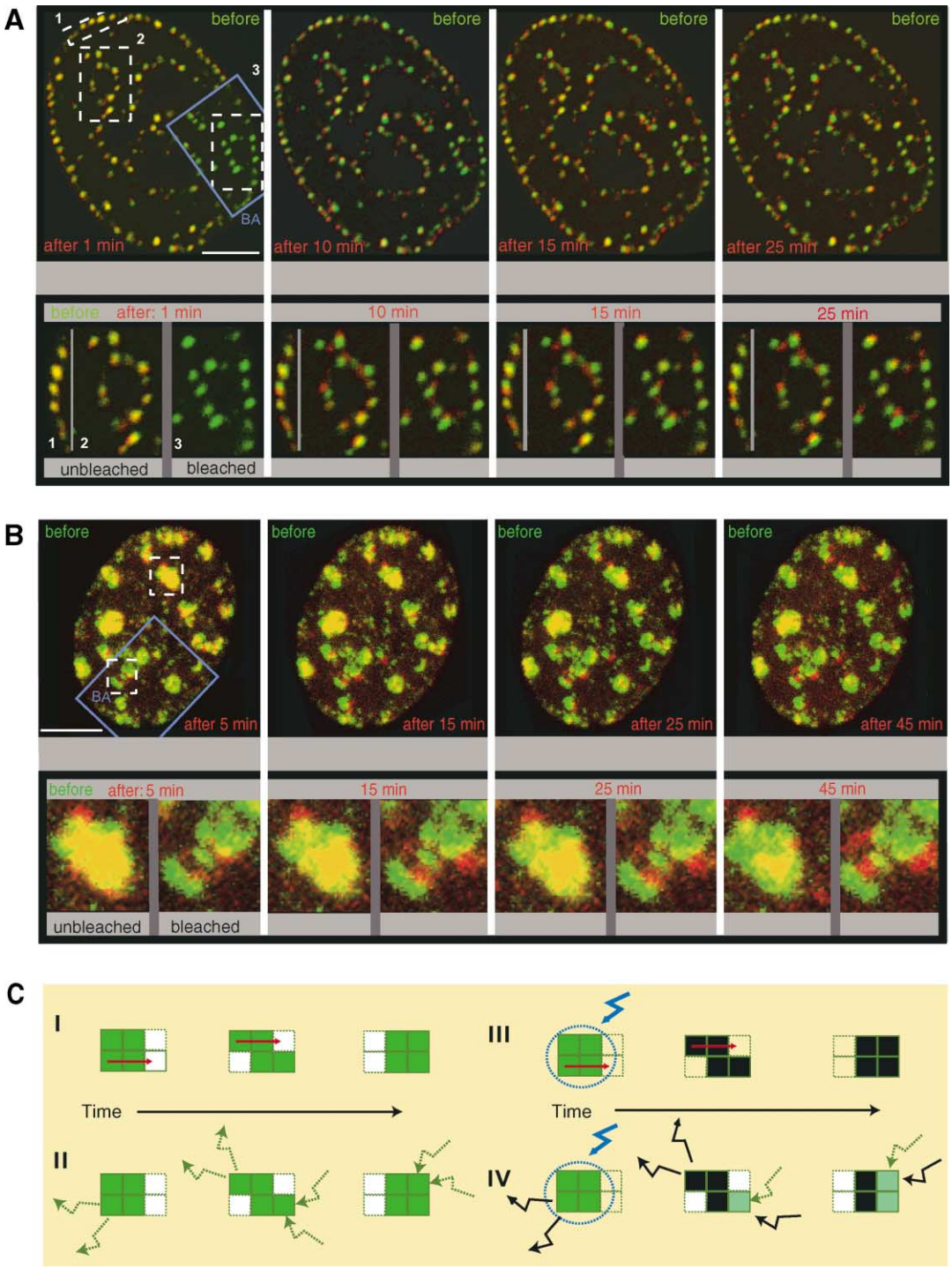

Figure 4. Replication Factors Are Not Directly Recycled to Newly Activated Adjacent Replicons

The spatial arrangement of GFP-PCNA replication foci before and after bleaching of an early/mid S phase nucleus (A) and a late S phase nucleus (B) was analyzed by time overlays. Confocal sections (A) or projections of z stacks (B) acquired before and after photobleaching were overlaid with green representing the initial image (before bleaching) and with red representing the different time points after bleaching. A set of selected regions (white boxes in [A] and [B]) within and outside the bleached area are shown at higher magnification. In both S phase stages, regain of fluorescence occurs not at the original foci but mostly at adjacent sites or in between prebleach foci, which are better seen in the magnified regions. In the unbleached area, the same is observed together with a decreasing overlay of foci existing before and after photobleaching, suggesting that fluorescent PCNA present initially dissociates slowly from the initial replication sites. (C) Shown are two possible models of how these temporal changes in shape and substructure of replication foci (clusters of green squares) could occur: (I) individual replisomes (green squares) with their subcomponents (replication factors) can move/relocate directly from one replicon to newly activated adjacent ones (shown as white squares turning green over time). Alternatively, replisomes can disassemble into their subcomponents, and replication factors diffusing in the nucleoplasmic pool (green arrows) can be recruited to assemble de novo at adjacent replicons (II). If mostly preassembled replisomes move, one would expect to see after photobleaching (blue arrow) no regain of fluorescence in adjacent areas (III). The contrary—a regain of fluorescence at adjacent sites—would be expected if mostly de novo assembly of replication factors from the nucleoplasm would take place (IV). Since a part of the nucleoplasmic and replication foci-associated GFP-PCNA is bleached, newly assembled replisomes are less bright. The time overlay analyses in this figure are compatible with the model shown in (II) and (IV).

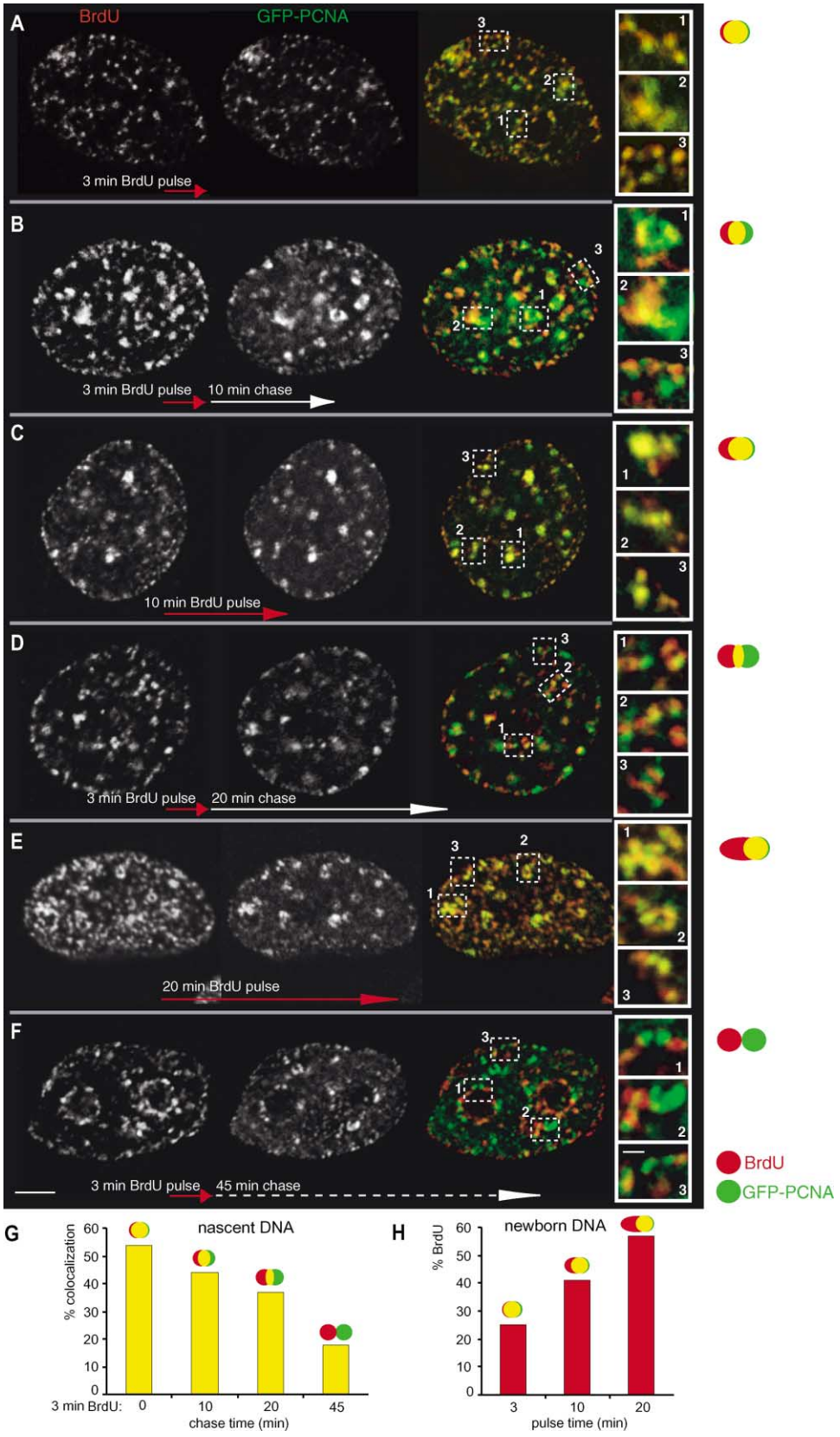

Figure 5. Spatial-Temporal Separation of GFP-PCNA from Newly Replicated DNA

C2C12 cells expressing GFP-PCNA were incubated for increasingly longer pulse times (3, 10, and 20 min; [A], [C], and [E], respectively) with the thymidine analog BrdU, fixed and stained with anti-BrdU antibody. The location of GFP-PCNA (green) at the end of the pulse time was

This recovery is slower than expected if a new PCNA ring is loaded for each Okazaki fragment. Therefore, we investigated the spatial distribution of the recovered fluorescence to determine when and where exactly new GFP-PCNA molecules were loaded.

Sequential Activation of Origin Clusters Occurs Preferentially Adjacent to Active Replication Foci, and Their Replisomes Are De Novo Assembled from the Nucleoplasmic Pool

We have previously shown that replication foci change in shape over time and contain distinct substructures revealed by deconvolution microscopy (Leonhardt et al., 2000). Those results raise the question whether these changes in shape were due to replication factors sliding along one replicon or directly moving from one replicon to newly activated adjacent ones or due to de novo assembly of diffusing replication factors from the nucleoplasmic pool.

To address this question we investigated the spatial distribution of the replication sites observed before and after bleaching of the early/mid S phase nucleus (Figure 4A) and the late S phase nucleus (Figure 4B) shown in Figure 3 and Supplemental Figure S1 at http://www.molecule.org/cgi/content/full/10/6/1355/DC1. Time overlays of either single confocal sections (Figure 4A) or projections of z stacks (Figure 4B) were performed in which the image before photobleaching is in green and the indicated time points after photobleaching in red. Thus, green areas represent foci that lost their fluorescence due to photobleaching or disassembly over time. Red areas represent foci that appeared after photobleaching, and yellow indicates areas where replication foci remained fluorescent in the unbleached area or recovered after bleaching. In both nuclei, the overall pattern of replication foci was relatively stable over time.

Notably, the regain of fluorescence in the bleached area did not directly occur at the replication sites visible before bleaching, but rather at adjacent locations with little to no overlap (Figure 4). This was true in both early/mid and late S phase nuclei, and it is shown for clarity at higher magnification. In particular, at the smaller foci of the early/mid S phase nucleus, the new sites filled the spaces between the prebleach ones (Figure 4A). This means that de facto there is little to no recovery of fluorescence but de novo assembly of new replication machines at preferentially adjacent locations. By contrast, the fast de novo assembly of GFP-RPA34 occurs at the prebleach replication sites, as shown by the yellow color in the time overlays in Figure 3B (insets). We can rule out systematic x, y, or z shifts of these images due to misalignment since new fluorescent sites appear in different directions within the same nucleus, at the same time. Furthermore, z stacks were acquired and analyzed at each time point to control for movements in and out of the focal plane. We can also exclude random shifts due to Brownian movements since the newly assembled foci (red spots in Figures 4A and 4B) do not change their position relative to the previous foci over time.

In the unbleached area, these overlays show that there is a substantial but, with time, decreasing colocalization of the unbleached foci before and after photobleaching. In the late S phase nucleus (Figure 4B) the size of the unbleached foci is clearly reduced by loss of fluorescence. Also, here a gain of fluorescence (in red) is visible in close vicinity to the prebleach foci. However, especially in the late S phase nucleus, some large unbleached foci remain fluorescent over 45 min, indicating active replication over this entire period. This likely occurs also in the bleached area but is not visible due to photobleaching.

To directly address whether GFP-PCNA labels active sites of DNA synthesis or whether a significant proportion of GFP-PCNA stays bound to postreplicative chromatin, we performed two complementary sets of experiments. In one we performed increasingly longer nucleotide pulse labeling (3, 10, and 20 min) and determined the relative proportion of "newborn" DNA no longer bound by GFP-PCNA as a function of labeling duration (Figure 2C [line scans] and Figures 5A, 5C, and 5E, quantification in 5H). The percent "newborn" DNA significantly increases over time, suggesting that the bulk GFP-PCNA is bound at the actively replicating sites (i.e., where "nascent" DNA is being synthesized). To more directly discriminate between "newborn" and "nascent" DNA, we performed a short nucleotide labeling pulse followed by increasingly longer chase times and determined the proportion of GFP-PCNA staying bound to the labeled DNA as a function of increasing chase duration (0, 10, 20, and 45 min; Figures 5A, 5B, 5D, and 5F, quantification in 5G). As predicted from the complementary set of experiments, the amount of GFP-PCNA which stays bound to previously replicated DNA decreases with increasing chase time, indicating that the bulk of GFP-PCNA labels active sites of DNA replication and is released from replicated DNA within about 20 min.

In summary, these results clearly demonstrate that replication foci show little to no exchange of PCNA, arguing against a constant loading of new PCNA rings

then determined in relation to the total amount of DNA (red) replicated during the pulse duration. For better visualization, magnified parts of the overlayed images are shown. The interpretation of the replication foci-labeling patterns is shown schematically on the side of each labeling scheme. Longer labeling times (C and E) lead to an increasing amount of labeled DNA, a subset of which colocalized with GFP-PCNA. This is also in agreement with the line intensity plot in Figure 2C on a 10 min pulse duration. The quantification in H shows an increase over time of the percent "newborn" DNA no longer bound by GFP-PCNA (red), suggesting that the bulk GFP-PCNA is bound at the actively replicating sites (i.e., where "nascent" DNA is being synthesized). To more directly address how long GFP-PCNA stays bound to newly replicated DNA, short BrdU-labeling pulses (3 min, [A]) were followed by chase times of increasing duration (0, 10, 20, and 45 min; [A], [B], [D], and [E], respectively) and analyzed as above. The quantification in (G), as predicted from the first of experiments, indicates that the amount of GFP-PCNA that stays bound to previously replicated DNA (yellow) decreases with increasing chase time. Since our percent colocalization is calculated taking into consideration all labeled pixels (green, red, or both), i.e., including also all green pixels in the image above background, we include the nucleoplasmic pool of GFP-PCNA and therefore do not get higher colocalization percentages. In summary, the bulk of GFP-PCNA labels sites of active replication and is released from replicated DNA within about 20 min (compare overlay images in [B] and [D]). Scale bar, 5 μm.

for each new Okazaki fragment. Instead, new sites become activated adjacent to existing foci and assemble replisomes from the nucleoplasmic pool.

Discussion

One of the remaining questions regarding the regulation and coordination of DNA replication in mammalian cells concerns the dynamics of the temporal and spatial organization of this process. We have previously shown that the pattern of nuclear replication foci undergoes defined changes throughout S phase, and that individual foci containing clusters of replisomes do not show directional movements (Leonhardt et al., 2000). To address the question how replication factor-labeled sites within the nucleus undergo this specific temporal change, we examined the diffusion and association properties of a central component of the DNA replication machinery, PCNA. Our results indicate that this replication factor diffuses through the nucleoplasm at a rate comparable to GFP alone (see Supplemental Figures S2E–S2H at http://www.molecule.org/cgi/content/full/10/6/1355/DC1) and gets transiently immobilized at replication sites (Figure 3 and Supplemental Figure S1 at http://www.molecule.org/cgi/content/full/10/6/1355/DC1). No evidence was found for a major fraction of GFP-PCNA being preassembled in the nucleoplasm into large complexes, such as replisomes. Similarly, GFP-tagged DNA repair factors were reported not to be present in large preassembled repair complexes by comparison to the diffusion of GFP alone (Houtsmuller et al., 1999). Since replication factors are sufficiently mobile in the nucleoplasm to reach their site of action by a stochastic process, they would not require any vectorial transport. Once bound to replication sites, GFP-PCNA does not exchange fast in and out of these structures as determined by photobleaching and in situ extraction experiments (Figures 1–3). Altogether these results indicate that replication foci are stable structures that are not in flux as proposed for the speckled compartment (Kruhlak et al., 2000; Phair and Misteli, 2000).

The function of PCNA as a DNA polymerase clamp and processivity factor clearly argues for a stable association throughout the replication of an entire replicon. However, the discontinuous nature of lagging strand synthesis and the multiple steps required for lagging strand maturation pose numerous challenges to a processive replication machinery. One possible solution would be to load a new PCNA ring for every Okazaki fragment as proposed before (Shibahara and Stillman, 1999). This would allow the replication fork to progress, while the PCNA ring is left behind to coordinate the next steps of lagging strand maturation. The principal models for lagging strand synthesis are outlined in a simplified version in Figure 6. The major differences in these models are whether or not a new PCNA ring is loaded for each Okazaki fragment and whether the new PCNA ring comes from the nucleoplasmic pool. In mammalian cells the replication fork progresses at an average rate of about 1.7 kbp per minute (Jackson and Pombo, 1998; reviewed in Berezney et al., 2000). This means that about 10 Okazaki fragments are synthesized per minute and would require the loading of about 10 PCNA trimers (30 PCNA molecules) per minute, if a new PCNA ring is loaded at each Okazaki fragment (Figure 6B). Since each replication focus seems to contain clusters of replicons (recent estimates in mammalian cells average 5 replicons per focus corresponding to 10 replication forks [Jackson and Pombo, 1998; Ma et al., 1998]), one would expect the loading of 300 PCNA molecules per minute at each replication focus. If, however, the PCNA ring remains associated with the replication machinery

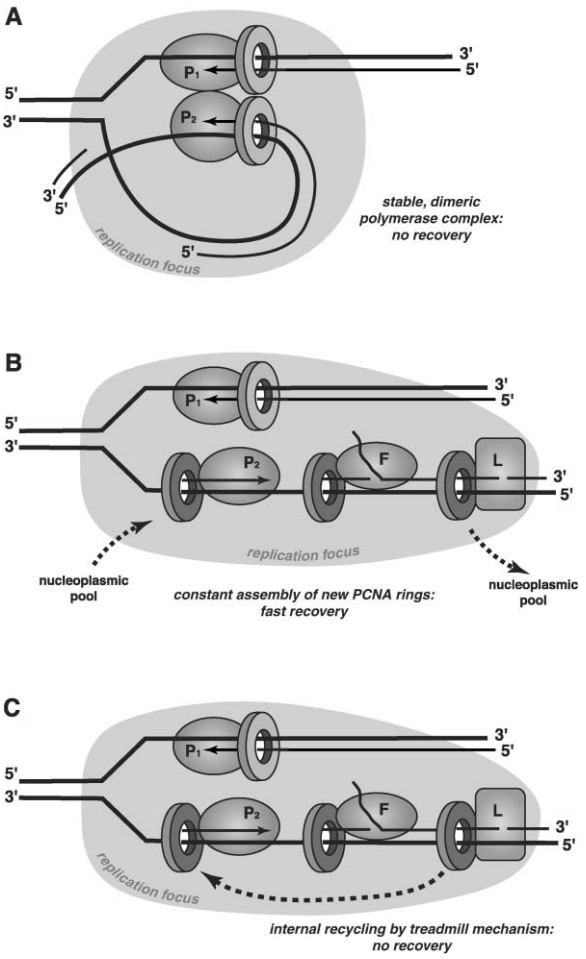

Figure 6. Models of PCNA Ring Dynamics at the Replication Fork

The lagging strand (P2) and leading strand (P1) polymerases are shown tethered to the DNA by a PCNA trimer (ring). The several other steps needed for maturation of the discontinuous lagging strand are here, for simplification, reduced to two, catalyzed by Fen1 (F) and DNA ligase I (L), and only one of the multiple replication forks is shown per focus. In (B) and (C), a new PCNA ring is loaded at each Okazaki fragment. In (B), after completion of one Okazaki fragment, the PCNA ring disassembles and is released into the nucleoplasmic pool, while a new one assembles at the next Okazaki fragment. As a result, a high turnover of PCNA is expected. Alternatively, in (C) the PCNA rings are internally recycled by a treadmill-like mechanism resulting in little to no turnover at the progressing replication fork. In (A), a modified dimeric polymerase model is shown, in which the lagging and leading strand polymerases as well as the respective PCNA rings are physically coupled. In this model, one PCNA ring would be reused over several Okazaki fragments cycling together with the polymerase to the next primer laid by polymerase α-primase. This would result in little to no turnover of PCNA at the lagging strand similar to the one for the leading strand.

through multiple rounds of Okazaki fragment synthesis, in a mode analogous to the cycling of the polymerase in the dimeric polymerase model (Figure 6A), one would expect a much slower turnover of PCNA. In an extreme case, any turnover would be limited to the loading of one ring each for leading and lagging strand and unloading upon completion.

Photobleaching experiments to measure the turnover of PCNA at individual replication foci showed that recovery occurred mostly at adjacent sites, with little or no regain of fluorescence at the replication focus itself, arguing strongly against a rapid turnover of PCNA at replication forks. We can rule out that this lack of recovery was caused by disrupting DNA replication (for example, by stalling at photodamaged sites) since the replication activity was unaltered by the photobleaching process (Figure 2). Likewise, we can exclude a critical depletion of the nucleoplasmic pool of fluorescent GFP-PCNA since new, fluorescent replisomes were assembled nearby (see red signal in Figures 4A and 4B). It is also rather improbable that in all the bleached foci, replication would have ceased and only postreplicative PCNA with a very slow exchange would be present. Our pulse and chase nucleotide-labeling experiments indicate that GFP-PCNA mostly associates at actively replicating DNA (Figures 2 and 5). Finally, the slow fluorescence recovery at bleached foci could be caused by reuse of nonfluorescent replication proteins within a focus. However, the fluorescence recovery of another replication protein (GFP-RPA34) shows a striking difference with PCNA: its fluorescence recovers at the bleached replication foci within seconds after photobleaching, whereas no recovery is seen with GFP-PCNA (Figure 3).

In summary, these results argue against a rapid turnover of PCNA at replication foci as would be expected if a new ring from the nucleoplasmic pool gets loaded for each Okazaki fragment (Figure 6B), and indicate instead a stable association with the replication machinery. Such a stable association could be achieved by coupling one PCNA ring to the leading strand polymerase/PCNA complex forming an asymmetric, dimeric polymerase complex (Figure 6A), which is reused for consecutive rounds of Okazaki fragment synthesis. Alternatively, PCNA rings could be left behind to coordinate the multiple steps of lagging strand synthesis, but would be internally recycled within the replisome by, for example, a treadmill-like mechanism (Figure 6C). In view of the biochemical data indicating accumulation of multiple rings at the lagging strand in prokaryotes (Stukenberg et al., 1994; Yuzhakov et al., 1996) and eukaryotes (Shibahara and Stillman, 1999), the latter model (Figure 6C) would best accommodate all the data. In this context it is interesting to notice that extracted cells continue to synthesize DNA (Jackson and Cook, 1986), pointing to the presence of higher order structures involved in organizing DNA replication in vivo that could play a role in the retention and reuse of PCNA at replication foci.

One of the still largely unsolved problems in DNA replication is the sequential activation of origins in mammalian cells. Each origin seems to have its specific and reproducible time of activation during S phase, which may change during development along with its transcriptional state (Goldman et al., 1984; Hatton et al., 1988). Since early origins tend to be transcriptionally active with an open chromatin structure, it is likely that chromatin accessibility is responsible for them being selected first during early S phase. The mechanism for the sequential activation of later origins, however, remained elusive.

By looking at the "regain" of GFP-PCNA fluorescence at replication sites after photobleaching, we found no detectable recovery of fluorescence but rather a de novo assembly of replisomes at adjacent sites throughout the nucleus, which is clearly shown in the higher magnification time overlays in Figure 4B. These data are perfectly consistent with previous studies where replicating chromatin was labeled by pulse-chase-pulse experiments with two different nucleotides. In these studies, cells were subsequently fixed and the incorporated nucleotides detected with specific antibodies either in situ (Berezney et al., 1995; Manders et al., 1996) or by DNA fiber fluorography (Jackson and Pombo, 1998). Furthermore, in the latter study, secondary replicon clusters were often activated adjacent to primary replicon clusters within a DNA fiber. In addition, by simultaneous time lapse analysis of GFP-PCNA-labeled foci and nascent DNA in living cells, we could observe the initial colocalization of replication proteins with nascent DNA and the subsequent appearance of GFP-PCNA-labeled foci adjacent to the previously replicated DNA (N. Sadoni et al., submitted).

An important point is that replication factors are not just sliding over from neighboring replisomes as outlined in Figure 4CI. Since regain of fluorescence is observed adjacent to photobleached sites, replication factors must be derived from the fast diffusing nucleoplasmic pool of fluorescent GFP-PCNA molecules as illustrated in Figure 4CII. Thus, the apparent small scale movement of replication sites observed by double DNA replication labeling (Ma et al., 1998; Manders et al., 1996) and by live cell imaging of replication factors (Leonhardt et al., 2000) is not due to local movement of replication machines but to de novo assembly of new replication factors from the nucleoplasmic pool (Figure 4).

The fact that most if not all newly assembled foci lie adjacent to earlier, active foci points to a mechanistic link between ongoing DNA replication and the activation of adjacent origin clusters. Since our photobleaching results clearly rule out a simple sliding or jumping of the replication machinery to adjacent origin clusters, the nature of activation has to be an indirect mechanism like a domino effect (Figure 4). We propose that this domino-effect-like activation of the "next-in-line" replicon cluster is a mechanism determining the temporal order of replication of the genome throughout S phase. At the beginning of S phase, a large number of replicon clusters are activated first maybe due to their transcriptionally active state and more accessible chromatin structure. From that time on, local destabilization or change of chromatin structure due to ongoing replication might activate neighboring clusters of origins and thus set up the spatial and temporal order of chromatin replication during S phase. The domino effect might also involve some large replicons lasting from early to late S phase (e.g., as described by Ermakova et al., 1999) that could provide a link between early and late replication sites. We have recently observed small scale chro-

matin reshuffling by high-resolution live cell microscopy where replication proteins and newly synthesized DNA were simultaneously analyzed (N. Sadoni et al., submitted). This local chromatin reshuffling could uncover and render accessible adjacent origins. Other mechanisms, such as repressive microenvironments around centromeres, may concomitantly play a role.

According to this domino effect model, the activation of the first origin clusters would start a chain reaction leading to the activation of later origin clusters depending on the relative spatial distribution of the genome within the nucleus. Since the latter seems mostly constant (Ferreira et al., 1997; Jackson and Pombo, 1998; Ma et al., 1998; Sparvoli et al., 1994; Zink et al., 1998, 1999), this would create a self-perpetuating system, maintaining the same temporal order of replication over cell generations until changes, likely epigenetic in nature, would alter chromatin structure, transcriptional activity, spatial distribution, and consequently the order of replication. Interestingly, a correlation between chromosome positioning in G1 and determination of the temporal order of genome replication was recently observed in a cell-free replication system (Dimitrova and Gilbert, 1999). Further quantitative studies on the dynamics of different replication factors are necessary to better understand the regulation of the replication of genetic and epigenetic information in mammalian cells. The photobleaching studies described here contribute the framework for a model of the sequential activation of replication origins in mammalian cells.

Experimental Procedures

GFP Fusion Proteins, Cell Culture, and Transfection

C2C12 mouse myoblast cells stably expressing either GFP-PCNAL2 (human PCNA [Leonhardt et al., 2000]) or enhanced GFP (pEGFPC1, Clontech) alone were established and grown as described (Leonhardt et al., 2000). The GFP-RPA34 fusion protein contains a SV40 nuclear localization signal at the NH_2 terminus followed by an enhanced GFP gene that is fused to the human RPA34 (the human RPA34 cDNA was provided by Marc S. Wold). Expression of the fusion protein is driven by the CMV promoter and the translation signals of the thymidine kinase gene, as is the case for GFP-PCNAL2 (pEVRF mammalian expression vector [Matthias et al., 1989]). C2C12 cells were transfected by the calcium phosphate-DNA coprecipitation method as described (Cardoso et al., 1997).

In Situ DNA Replication Assay (BrdU Labeling) and Immunofluorescence Analysis

Cells grown on glass coverslips or labtek chambered coverslips (Nunc) were pulse labeled for 3–20 min with 20 μM BrdU (Sigma) at 37°C. Cells were fixed with 3.7% formaldehyde in PBS for 10 min at room temperature either immediately after labeling or after varying chase times (10–45 min). Chase was performed by washing cells twice with 200 μM thymidine and growing them in conditioned cell culture medium. Fixed cells were permeabilized with 0.5% Triton-X 100 in PBS for 10 min and blocked in 0.2% fish skin gelatin solution in PBS (blocking buffer) for 30 min. Incorporated BrdU was detected with a mouse monoclonal anti-BrdU antibody (Becton-Dickinson) and the epitope exposed by incubating with 20 U/ml DNase I (Boehringer Mannheim) for 30 min at 37°C followed by anti-mouse IgG antibody conjugated with AlexaFluor568 (Molecular Probes). Endogenous PCNA was detected in methanol-fixed C2C12 cells with a mouse monoclonal anti-PCNA antibody (clone PC 10, Dako) followed by anti-mouse IgG antibody conjugated with AlexaFluor568 (Molecular Probes). Antibodies were diluted in blocking buffer. Stacks of confocal images (350 nm optical slices) were acquired with a confocal laser scanning microscope LSM510 (Zeiss). GFP and AlexaFluor568 were excited at 488 and 543 nm, respectively, and detected with a 500–530 nm band pass and a 560 nm long pass filter, respectively. Acquisition was performed sequentially to prevent bleedthrough.

In Situ Salt Extractions

Cells grown on coverslips were permeabilized for about 30 s with ice-cold CSK buffer (50 mM NaCl, 250 mM sucrose, 2 mM $MgCl_2$, 2 mM EGTA, 10 mM PIPES, pH 6.8) containing 0.1% Triton-X 100. Thereafter, the permeabilized cells were extracted for 1 min with ice-cold phosphate buffer containing different NaCl concentrations (150, 300, and 500 mM). Unextracted (control) and salt-extracted cells were fixed for 5 min with ice-cold methanol. C2C12 parental cells were then immunostained for endogenous PCNA as described above. Immunofluorescence staining was not performed on the cell line expressing the GFP fusion protein since the antibody would not only recognize the endogenous but also the GFP fusion protein.

Live Cell Microscopy and Fluorescence Recovery after Photobleaching (FRAP)

For live cell microscopy, cells were grown on 40 mm diameter glass coverslips and kept in a FCS2 live cell microscopy chamber (Bioptechs) at 37°C as described (Leonhardt et al., 2000). FRAP experiments were performed on a LSM510 using a 63× NA 1.4 Planapochromat oil immersion objective (Zeiss) with a 488 nm laser line. Laser power for observation was typically 1%–5%, and care was taken to prevent oversaturation of images. After acquisition of an initial (prebleach) z stack, a part of a middle z plane of the nucleus was bleached for 2 s by increasing the laser power to 100% at increased magnification. Thereafter, confocal z stacks (postbleach) with the initial settings were acquired for various times and intervals. Up to one-third of total fluorescence was lost due to the photobleaching event, and further 10%–15% loss typically occurred during the subsequent acquisition of image z stacks.

Image Analysis and Data Processing

Series of images were corrected for cellular movements and focal drift. Projections of z stacks were produced with Confocal Assistant 4.0 (T.C. Brelje). Adobe Photoshop 5.5 and Zeiss LSM510 software were used for quantification of fluorescence intensities (mean fluorescence intensity of an area or fluorescence intensities along a line). Chosen areas were kept constant for all time points and all foci within the same nucleus. For colocalization analysis, images were correlated after thresholding and converting to binary images in Image J 1.28e (NIH). Diagrams were generated with Microsoft Excel 5.0. Adobe Photoshop 5.5 and Adobe Illustrator 8.0 were used to assemble and annotate all figures.

Acknowledgments

We thank Hans-Peter Rahn for help and Hariharan P. Easwaran for many stimulating discussions. The human RPA34 cDNA was kindly provided by Mark S. Wold. A.G. was supported by the European Union (ESF Program). This work was funded by the Deutsche Forschungsgemeinschaft.

Received: March 3, 2002
Revised: September 19, 2002

References

Berezney, R., Ma, H., Meng, C., Samarabandu, J., and Cheng, P.-C. (1995). Connecting genomic architecture and DNA replication in three dimensions. Zool. Stud. *34*, 29–32.

Berezney, R., Dubey, D.D., and Huberman, J.A. (2000). Heterogeneity of eukaryotic replicons, replicon clusters, and replication foci. Chromosoma *108*, 471–484.

Boudonck, K., Dolan, L., and Shaw, P.J. (1999). The movement of coiled bodies visualized in living plant cells by the green fluorescent protein. Mol. Biol. Cell *10*, 2297–2307.

Cardoso, M.C., Joseph, C., Rahn, H.P., Reusch, R., Nadal-Ginard, B., and Leonhardt, H. (1997). Mapping and use of a sequence that

targets DNA ligase I to sites of DNA replication in vivo. J. Cell Biol. *139*, 579–587.

Dimitrova, D.S., and Gilbert, D.M. (1999). The spatial position and replication timing of chromosomal domains are both established in early G1 phase. Mol. Cell *4*, 983–993.

Ermakova, O.V., Nguyen, L.H., Little, R.D., Chevillard, C., Riblet, R., Ashouian, N., Birshtein, B.K., and Schildkraut, C.L. (1999). Evidence that a single replication fork proceeds from early to late replicating domains in the IgH locus in a non-B cell line. Mol. Cell *3*, 321–330.

Ferreira, J., Paolella, G., Ramos, C., and Lamond, A.I. (1997). Spatial organization of large-scale chromatin domains in the nucleus: a magnified view of single chromosome territories. J. Cell Biol. *139*, 1597–1610.

Goldman, M.A., Holmquist, G.P., Gray, M.C., Caston, L.A., and Nag, A. (1984). Replication timing of genes and middle repetitive sequences. Science *224*, 686–692.

Gulbis, J.M., Kelman, Z., Hurwitz, J., O'Donnell, M., and Kuriyan, J. (1996). Structure of the C-terminal region of p21(WAF1/CIP1) complexed with human PCNA. Cell *87*, 297–306.

Hatton, K.S., Dhar, V., Brown, E.H., Iqbal, M.A., Stuart, S., Didamo, V.T., and Schildkraut, C.L. (1988). Replication program of active and inactive multigene families in mammalian cells. Mol. Cell. Biol. *8*, 2149–2158.

Houtsmuller, A.B., Rademakers, S., Nigg, A.L., Hoogstraten, D., Hoeijmakers, J.H., and Vermeulen, W. (1999). Action of DNA repair endonuclease ERCC1/XPF in living cells. Science *284*, 958–961.

Huberman, J.A., and Riggs, A.D. (1968). On the mechanism of DNA replication in mammalian chromosomes. J. Mol. Biol. *32*, 327–341.

Hubscher, U., and Seo, Y.S. (2001). Replication of the lagging strand: a concert of at least 23 polypeptides. Mol. Cells *12*, 149–157.

Jackson, D.A., and Cook, P.R. (1986). Replication occurs at a nucleoskeleton. EMBO J. *5*, 1403–1410.

Jackson, D.A., and Pombo, A. (1998). Replicon clusters are stable units of chromosome structure: evidence that nuclear organization contributes to the efficient activation and propagation of S phase in human cells. J. Cell Biol. *140*, 1285–1295.

Krishna, T.S., Kong, X.P., Gary, S., Burgers, P.M., and Kuriyan, J. (1994). Crystal structure of the eukaryotic DNA polymerase processivity factor PCNA. Cell *79*, 1233–1243.

Kruhlak, M.J., Lever, M.A., Fischle, W., Verdin, E., Bazett-Jones, D.P., and Hendzel, M.J. (2000). Reduced mobility of the alternate splicing factor (ASF) through the nucleoplasm and steady state speckle compartments. J. Cell Biol. *150*, 41–51.

Lee, J., Chastain, P.D., 2nd, Kusakabe, T., Griffith, J.D., and Richardson, C.C. (1998). Coordinated leading and lagging strand DNA synthesis on a minicircular template. Mol. Cell *1*, 1001–1010.

Leonhardt, H., Rahn, H.P., Weinzierl, P., Sporbert, A., Cremer, T., Zink, D., and Cardoso, M.C. (2000). Dynamics of DNA replication factories in living cells. J. Cell Biol. *149*, 271–280.

Lima-de-Faria, A., and Jaworska, H. (1968). Late DNA synthesis in heterochromatin. Nature *217*, 138–142.

Ma, H., Samarabandu, J., Devdhar, R.S., Acharya, R., Cheng, P., Meng, C., and Berezney, R. (1998). Spatial and temporal dynamics of DNA replication sites in mammalian cells. J. Cell Biol. *143*, 1415–1425.

Manders, E.M., Stap, J., Strackee, J., van Driel, R., and Aten, J.A. (1996). Dynamic behavior of DNA replication domains. Exp. Cell Res. *226*, 328–335.

Matthias, P., Müller, M.M., Schreiber, E., Rusconi, S., and Schaffner, W. (1989). Eukaryotic expression vectors for the analysis of mutant proteins. Nucleic Acids Res. *17*, 6418.

McHenry, C.S. (1988). DNA polymerase III holoenzyme of Escherichia coli. Annu. Rev. Biochem. *57*, 519–550.

Misteli, T. (2001). Protein dynamics: implications for nuclear architecture and gene expression. Science *291*, 843–847.

Nakamura, H., Morita, T., and Sato, C. (1986). Structural organizations of replicon domains during DNA synthetic phase in the mammalian nucleus. Exp. Cell Res. *165*, 291–297.

Noguchi, H., Prem veer Reddy, G., and Pardee, A.B. (1983). Rapid incorporation of label from ribonucleoside disphosphates into DNA by a cell-free high molecular weight fraction from animal cell nuclei. Cell *32*, 443–451.

Pederson, T. (2000). Diffusional protein transport within the nucleus: a message in the medium. Nat. Cell Biol. *2*, E73–E74.

Phair, R.D., and Misteli, T. (2000). High mobility of proteins in the mammalian cell nucleus. Nature *404*, 604–609.

Prelich, G., and Stillman, B. (1988). Coordinated leading and lagging strand synthesis during SV40 DNA replication in vitro requires PCNA. Cell *53*, 117–126.

Schurtenberger, P., Egelhaaf, S.U., Hindges, R., Maga, G., Jonsson, Z.O., May, R.P., Glatter, O., and Hubscher, U. (1998). The solution structure of functionally active human proliferating cell nuclear antigen determined by small-angle neutron scattering. J. Mol. Biol. *275*, 123–132.

Shibahara, K., and Stillman, B. (1999). Replication-dependent marking of DNA by PCNA facilitates CAF-1-coupled inheritance of chromatin. Cell *96*, 575–585.

Shopland, L.S., and Lawrence, J.B. (2000). Seeking common ground in nuclear complexity. J. Cell Biol. *150*, F1–F4.

Sinha, N.K., Morris, C.F., and Alberts, B.M. (1980). Efficient in vitro replication of double-stranded DNA templates by a purified T4 bacteriophage replication system. J. Biol. Chem. *255*, 4290–4293.

Sleeman, J.E., and Lamond, A.I. (1999). Newly assembled snRNPs associate with coiled bodies before speckles, suggesting a nuclear snRNP maturation pathway. Curr. Biol. *9*, 1065–1074.

Somanathan, S., Suchyna, T., Siegel, A., and Berezney, R. (2001). Targeting of PCNA to sites of DNA replication in the mammalian cell nucleus. J. Cell. Biochem. *81*, 56–67.

Sparvoli, E., Levi, M., and Rossi, E. (1994). Replicon clusters may form structurally stable complexes of chromatin and chromosomes. J. Cell Sci. *107*, 3097–3103.

Stukenberg, P.T., Turner, J., and O'Donnell, M. (1994). An explanation for lagging strand replication: polymerase hopping among DNA sliding clamps. Cell *78*, 877–887.

Tom, T.D., Malkas, L.H., and Hickey, R.J. (1996). Identification of multiprotein complexes containing DNA replication factors by native immunoblotting of HeLa cell protein preparations with T-antigen-dependent SV40 DNA replication activity. J. Cell. Biochem. *63*, 259–267.

Tsurimoto, T., and Stillman, B. (1989). Multiple replication factors augment DNA synthesis by the two eukaryotic DNA polymerases, alpha and delta. EMBO J. *8*, 3883–3889.

Waga, S., and Stillman, B. (1994). Anatomy of a DNA replication fork revealed by reconstitution of SV40 DNA replication in vitro. Nature *369*, 207–212.

Wu, C.A., Zechner, E.L., Hughes, A.J., Jr., Franden, M.A., McHenry, C.S., and Marians, K.J. (1992). Coordinated leading- and lagging-strand synthesis at the Escherichia coli DNA replication fork. IV. Reconstitution of an asymmetric, dimeric DNA polymerase III holoenzyme. J. Biol. Chem. *267*, 4064–4073.

Wu, Y., Hickey, R., Lawlor, K., Wills, P., Yu, F., Ozer, H., Starr, R., Quan, J.Y., Lee, M., and Malkas, L. (1994). A 17S multiprotein form of murine cell DNA polymerase mediates polyomavirus DNA replication in vitro. J. Cell. Biochem. *54*, 32–46.

Yuzhakov, A., Turner, J., and O'Donnell, M. (1996). Replisome assembly reveals the basis for asymmetric function in leading and lagging strand replication. Cell *86*, 877–886.

Zink, D., Bornfleth, H., Visser, A., Cremer, C., and Cremer, T. (1999). Organization of early and late replicating DNA in human chromosome territories. Exp. Cell Res. *247*, 176–188.

Zink, D., Cremer, T., Saffrich, R., Fischer, R., Trendelenburg, M.F., Ansorge, W., and Stelzer, E.H. (1998). Structure and dynamics of human interphase chromosome territories in vivo. Hum. Genet. *102*, 241–251.

Supplementary figures:

Fig. S1: Transient Immobilization of GFP-PCNA at Replication Sites
An area containing several GFP-PCNA foci (blue square, BA) was bleached in an early/mid S-phase nucleus (A) or in a late S-phase nucleus (B) of living C2C12 cells. Confocal z-stacks of the nucleus before and at several time points after photobleaching were acquired. In both experiments, single confocal sections are shown. Scale bars, 5 m. Fluorescence intensity change of several replication foci over time was analyzed in the early/mid S-phase (diagram C) and the late S-phase nucleus (diagram D). For quantification, the mean fluorescence intensity of the respective focus was determined at all time points and the initial value (i.e., before bleaching) of the brightest focus (focus 4) was set to 1. Foci 1 and 2 are located in the bleached area; foci 3 and 4 are located in the unbleached area. At the first time point after bleaching (<1 min) the fluorescence in the bleached areas is strongly reduced to the nucleoplasmic level while fluorescence in the unbleached area is moderately reduced (diagram C) or unchanged (diagram D). At the following time points, the fluorescence in the bleached areas increases constantly but non-uniformly (except at 25 min in C) while the fluorescence in the unbleached area decreases constantly but nonuniformly. In a typical experiment, up to 30% of GFP-PCNA was bleached due to bleaching event and 10–15% due to image acquisition. As compared to the very rapid recovery of fluorescence in the nucleoplasmic pool (Supplemental Figure S2), this indicates a transient immobilization of GFP-PCNA at replication foci.

Fig. S2: Rapid Diffusion and High Mobility of Nucleoplasmic GFP-PCNA in Non S-Phase and S-Phase Nuclei Measured by Fluorescence Loss in Photobleaching (FLIP) and FRAP(A–D) In non S-phase nuclei expressing GFP-PCNA, we performed FLIP experiments by repeated photobleaching (six times for about 2 s) of one small area (bleached area, BA) of the nucleus with an image acquired after each bleaching event. An almost complete depletion of fluorescence was observed indicating a very high population of mobile GFP-PCNA in the nucleus of non S-phase cells. (C) The amount of fluorescence after each bleaching event shows a nonlinear loss of fluorescence in the live cell nucleus caused by a dilution effect due to the limited number of fluorophores in the nucleus. 90 min after the end of the bleaching procedure, a small regain in nuclear fluorescence was observed, probably due to de novo synthesis of GFP-PCNA in the living cells. In formaldehyde fixed cells (B), one single bleaching event already reduced the fluorescence to background level. No substantial loss of fluorescence in adjacent areas and neighboring cells was found due to the bleaching procedure (quantification not shown). No recovery of fluorescence was observed in the fixed cell 90 min after end of photobleaching, indicating irreversible fluorophore inactivation. Projections of confocal z-stacks are shown in the fixed cell experiment, demonstrating that photobleaching in one z-section results in loss of fluorescence in all z-sections of the stack. Scale bar, 10 m.(E-H) To further investigate the mobility of nucleoplasmic GFP-PCNA, high-speed FRAP experiments were performed on an LSM 510 (Zeiss) equipped with an argon laser (15 mW) using a 63×NA 1.4 Planapochromat oil immersion objective. A small area of about 1 m2 within the nucleus was bleached for 0.35 s with 100% laser power. Before and after photobleaching, the fluorescence intensity of the bleached area (BA) and one control area

(CA) was measured every 20 ms with the time course feature of the Zeiss LSM 510 software (12-bit mode). A typical experimental setup is shown for a non S-phase nucleus (E) and for an S-phase nucleus (G). Scale bars, 5 m. Diagram F compares the fluorescence recovery of nucleoplasmic GFP (gray) to GFP-PCNA in non S-phase nuclei (black). An almost complete recovery of both proteins is observed with a faster diffusion of GFP (diffusion coefficient D = 2.8 m2/s) followed by GFP-PCNA (D = 1.7 m2/s). Diagram H compares the fluorescence recovery of nucleoplasmic GFP-PCNA in S-phase nuclei (gray) with the recovery of GFP-PCNA in non S-phase nuclei (black). No significant differences in the recovery dynamics of nucleoplasmic GFP-PCNA in S-phase and non S-phase nuclei are found. Each curve represents a mean of five to eight experiments in different nuclei. Microcal Origin 4.0 was used for calculations on FRAP curves. Curves were background corrected and with the help of the fluorescence intensity of the control area corrected for the overall loss of fluorescence due to the bleaching event. Diffusion coefficients (D) and half time of recovery (t1/2) were calculated with the 3-point fit approach (Axelrod et al., 1976), giving a rough estimation of these parameters.

Fig. S3: Characterization of the GFP-RPA34 Fusion Protein (A) Structure and expected size of the GFP-RPA34 fusion protein. The GFP-RPA34 fusion protein contains a SV40 nuclear localisation signal at the NH2 terminus followed by an enhanced mutant GFP gene that is fused to the human RPA34. (B) Western Blot analysis of the GFP fusion protein expressed in COS7 cells. COS7 cells were cultivated in DMEM containing 10% fetal calf serum and transiently transfected by the DEAE pretreatment method as described (Leonhardt et al., 1992). Whole-cell extracts were separated by 10% SDS-PAGE under reducing conditions and transferred to PVDF membranes. After incubation with rabbit polyclonal anti-GFP antibody (Abcam) or mouse monoclonal anti-RPA34 antibody (Oncogene) followed by HRP-conjugated secondary antibodies (Amersham), the blots were developed using ECL+ detection procedure (Amersham). Both antibodies detect a protein band of the expected size in transfected cells but not in untransfected (mock) cultures and in addition the anti-RPA34 antibody reveals the endogenous RPA34. Molecular weight markers are indicated om each side of the blots in kDa. (C) Immunofluorescence analysis shows that GFP-RPA34 expressed in C2C12 mouse myoblast cells localizes to sites of ongoing DNA replication visualized by incorporated BrdU or endogenous PCNA.

Figure S1:

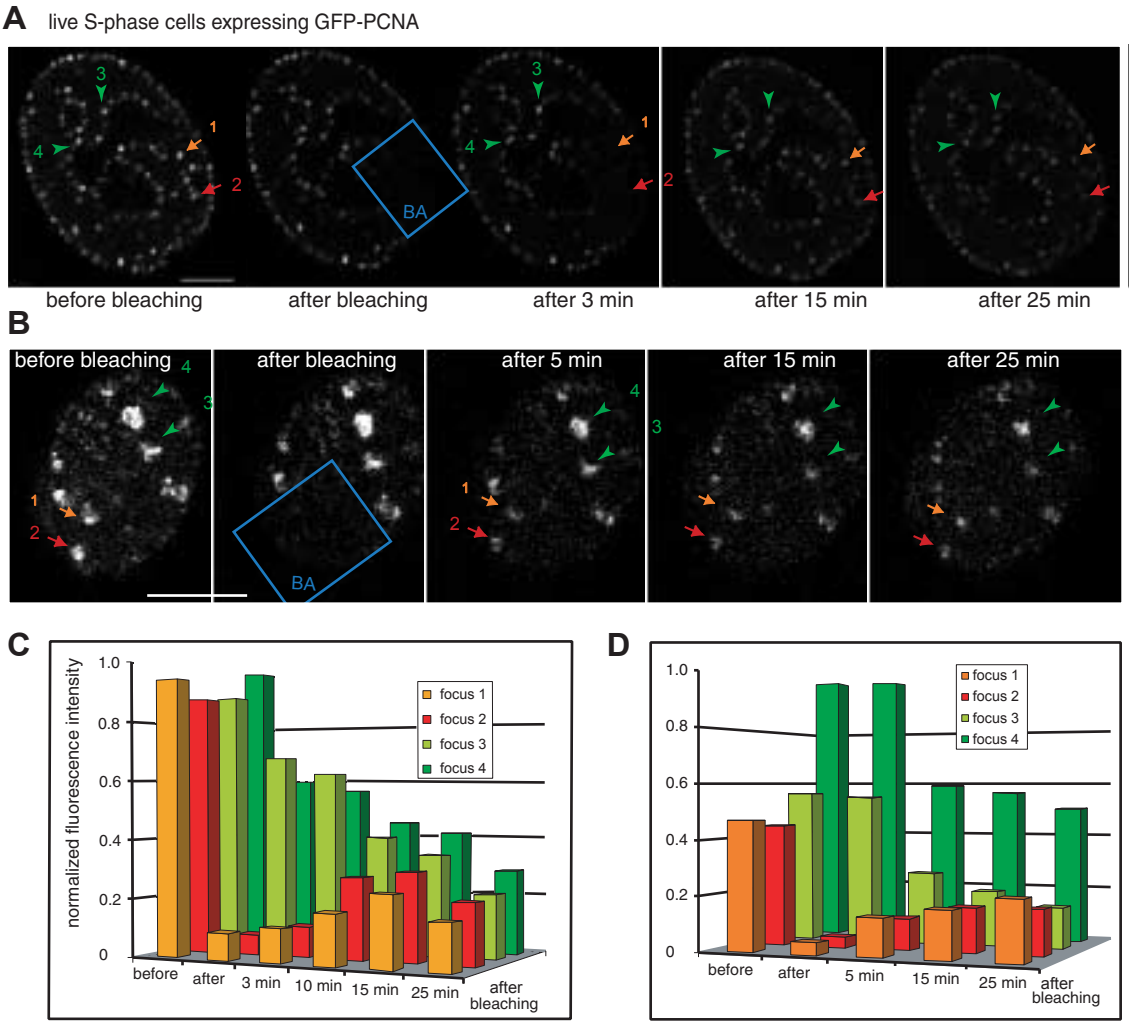
A
live S-phase cells expressing GFP-PCNA
3
1
4
2
BA
before bleaching
after bleaching
after 3 min
after 15 min
after 25 min
B
before bleaching
after bleaching
after 5 min
after 15 min
after 25 min
BA
C
normalized fluorescence intensity
1.0
0.8
0.6
0.4
0.2
0
focus 1
focus 2
focus 3
focus 4
before
after
3 min
10 min
15 min
25 min
after bleaching
D
1.0
0.8
0.6
0.4
0.2
0
focus 1
focus 2
focus 3
focus 4
before
after
5 min
15 min
25 min
after bleaching

Figure S2:

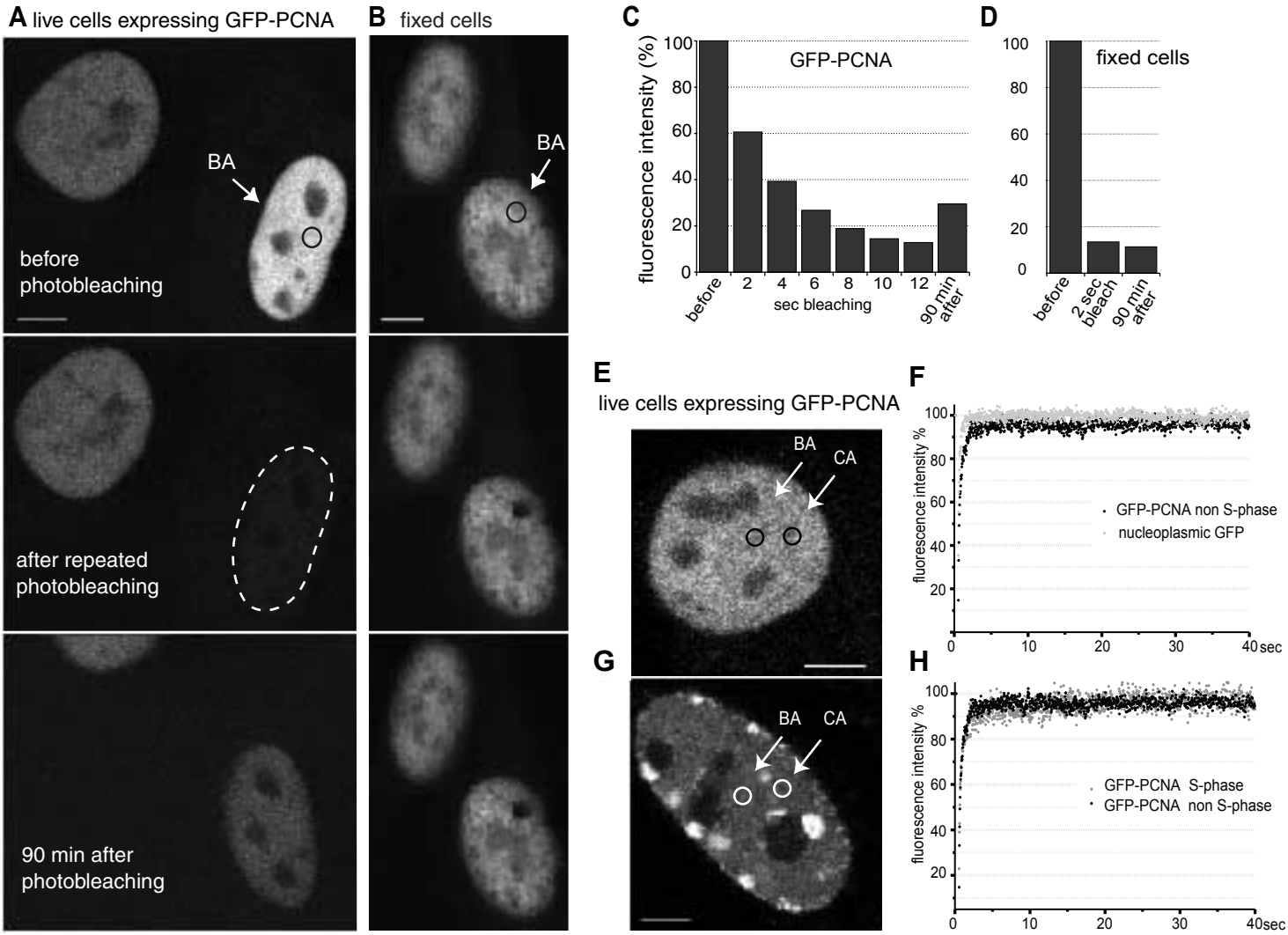
A live cells expressing GFP-PCNA
B fixed cells
BA
before photobleaching
after repeated photobleaching
90 min after photobleaching
C
GFP-PCNA
fluorescence intensity (%)
sec bleaching
before
90 min after
D
fixed cells
2 sec bleach
E
live cells expressing GFP-PCNA
CA
F
GFP-PCNA non S-phase
nucleoplasmic GFP
fluorescence intensity %
sec
G
H
GFP-PCNA S-phase
GFP-PCNA non S-phase

Figure S3:

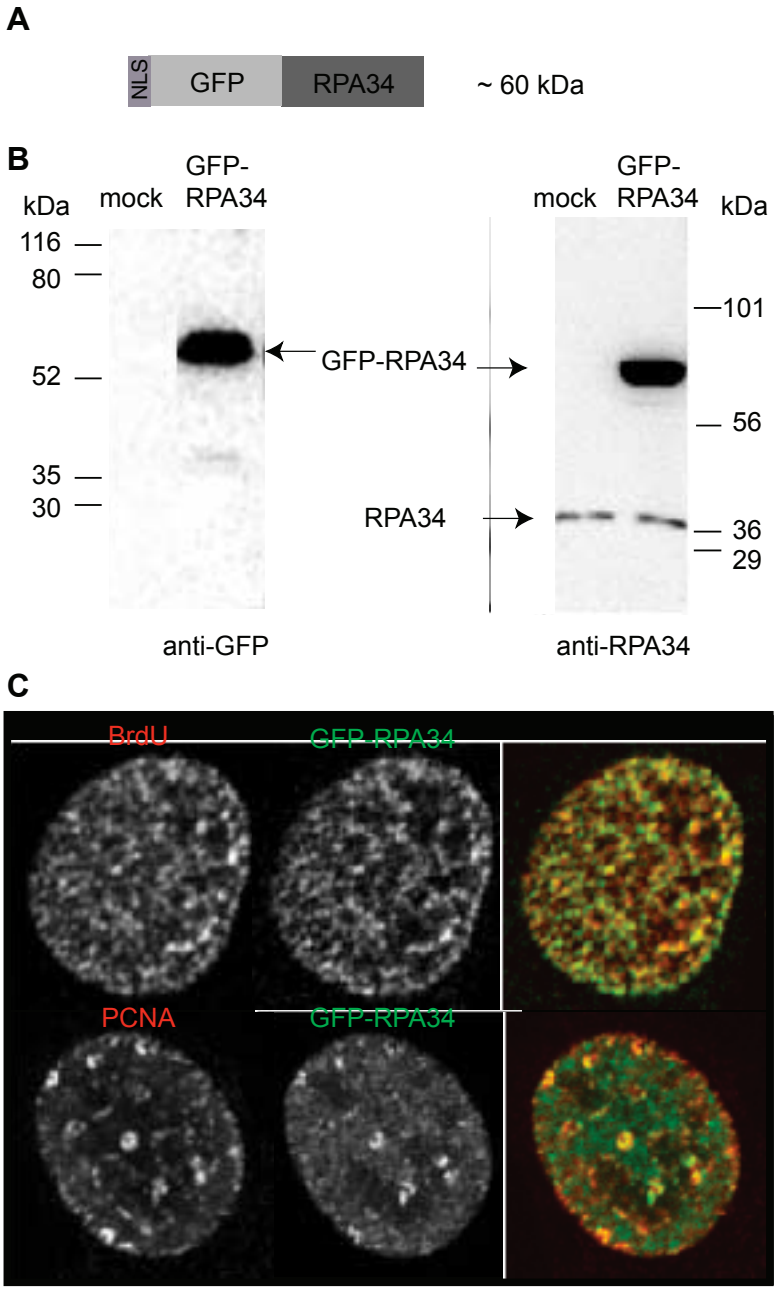
A
NLS
GFP
RPA34
~ 60 kDa
B
kDa
mock
GFP-RPA34
116
80
52
35
30
GFP-RPA34
RPA34
mock
GFP-RPA34
kDa
101
56
36
29
anti-GFP
anti-RPA34
C
BrdU
GFP-RPA34
PCNA
GFP-RPA34